

Glucosyl-1*H*-imidazole: A New Class of Azole-Type β -Glucosidase Inhibitor

Sybrin P. Schröder,[†] Liang Wu,[§] Marta Artola,[†] Thomas Hansen,[†] Wendy A. Offen,[§] Maria J. Ferraz,[‡] Kah-Yee Li,[†] Johannes M. F. G. Aerts,[‡] Gijsbert A. van der Marel,[†] Jeroen D. C. Codée,[†] Gideon J. Davies,[§] and Herman S. Overkleeft^{*,†}

[†]Department of Bioorganic Synthesis and [‡]Department of Medical Biochemistry, Leiden Institute of Chemistry, Leiden University, Einsteinweg 55, 2333 CC Leiden, The Netherlands

[§]Department of Chemistry, York Structural Biology Laboratory, University of York, Heslington, York YO10 5DD, United Kingdom

Supporting Information

ABSTRACT: Gluco-azoles competitively inhibit glucosidases by transition-state mimicry and their ability to interact with catalytic acid residues in glucosidase active sites. We noted that no azole-type inhibitors described, to date, possess a protic nitrogen characteristic for 1*H*-imidazoles. Here, we present glucosyl-1*H*-imidazole, a glucosyl-azole bearing a 1*H*-imidazole fused to a glucopyranose-configured cyclitol core, and three close analogues as new glucosidase inhibitors. All compounds inhibit human retaining β -glucosidase, GBA1, with the most potent ones inhibiting this enzyme (deficient in Gaucher disease) on a par with glucoimidazole. None inhibit glucosylceramide synthase, cytosolic β -glucosidase GBA2 or α -glucosidase GAA. Structural, physical and computational studies provide first insights into the binding mode of this conceptually new class of retaining β -glucosidase inhibitors.

Glucosidases catalyze the hydrolysis of interglycosidic linkages, and glucosidase inhibitors are widely regarded as promising therapeutic entities.¹ Azole-containing glycopyranoside mimics are a major class of competitive glucosidase inhibitors.² The natural product, nagstatin (**1**), is a potent *N*-acetyl- β -D-glucosaminidase (NAG) inhibitor.³ Glucopyranose mimics bearing tetrazole (**2**), triazole (**3**, **4**) and imidazole (**5**) moieties have been conceived as β -glucosidase inhibitors by Tatsuta and Vasella, with inhibitory potencies against sweet almond β -glucosidase ranging from low nanomolar (**5**) to high micromolar (**4**, Figure 1a).^{4–7} The reaction itinerary followed by many β -glucosidases proceeds via a ⁴H₃ transition state conformation,⁸ matching one of the thermodynamically most favored conformations of gluco-azoles (local minima calculated for **5** are ⁴H₃ and ³H₄).⁹ This conformational transition state mimicry contributes considerably to the inhibitory potency of gluco-azoles. Vasella concluded, from extensive studies on gluco-azoles (including compounds **2–5**), that an azole nitrogen at the position corresponding to the exocyclic oxygen in a β -glucoside substrate is essential for inhibitory potency, as this “exocyclic” nitrogen participates in lateral coordination with the catalytic acid/base of antiprotonating glucosidases.^{10–14} Remarkably, no azole-type inhibitors synthesized

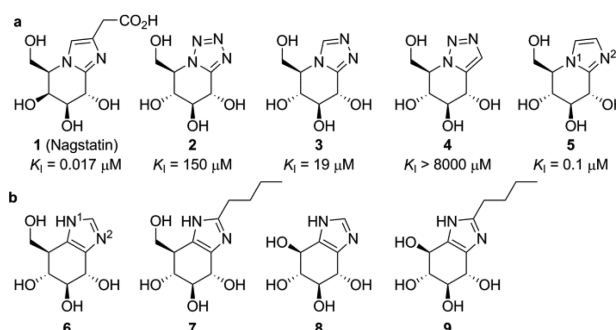


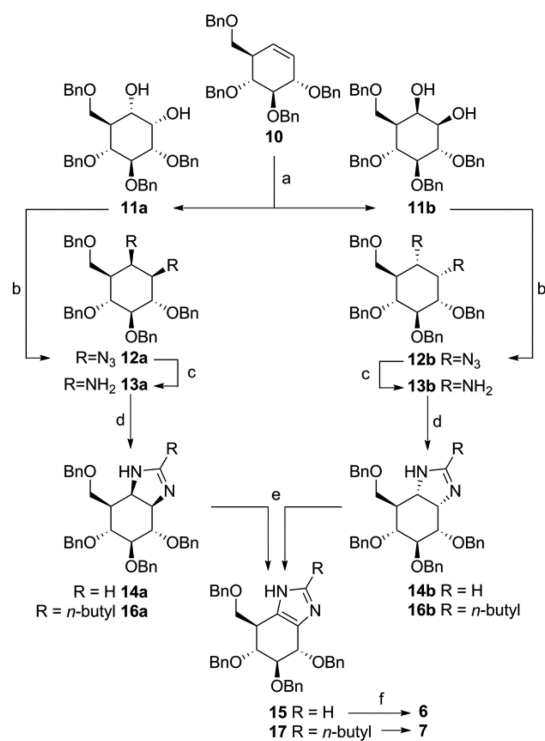
Figure 1. (a) Known cyclitol-azole type glycosidase inhibitors and their inhibitory potencies against porcine NAG (**1**)³ and sweet almond β -glucosidase (**2–5**).^{4–7} (b) 1*H*-Imidazoles subject of this study.

to date are protic with respect to the azole ring (such as 1*H*-imidazoles), and we reasoned that such positional isomers would be attractive alternatives to the reported gluco-azoles. Herein, we report on the synthesis and biochemical evaluation of gluco-1*H*-imidazole **6** and its analogues **7–9** as conceptually new retaining β -glucosidase inhibitors (Figure 1b).

The synthesis of gluco-1*H*-imidazole **6** commenced with cyclohexene **10**,¹⁵ which was transformed into the vicinal diamine following a modified procedure from Lleberia (Scheme 1).¹⁶ Rapid conversion of **10** was accomplished using RuCl₃/NaIO₄, affording a separable, near equimolar mixture of 1,2-*cis*-dihydroxy isomers **11a** (*S,S*) and **11b** (*R,R*).¹⁷ Bismesylation and subsequent azide substitution afforded diazido cyclitols **12a,b**. Platinum oxide catalyzed hydrogenolysis afforded diamino cyclitols **13a,b**, which were condensed with trimethyl orthoformate in hexafluoroisopropanol (HFIP) to afford imidazolines **14a,b**.¹⁸ Protected 1*H*-imidazole **15** was obtained by oxidation of either isomer of **14** with IBX/DMSO,¹⁹ and final hydrogenolysis afforded gluco-1*H*-imidazole **6**. Derivatization of the imidazole ring of gluco-1*H*-imidazoles was achieved by variation of the trimethyl orthoester employed. Thus, reaction of **13a,b** with trimethyl orthovalerate followed by oxidation and deprotection furnished 2-butyl-1*H*-imidazole **7** via **16a,b** and **17**. Utilizing tetrabenzyl *myo*-diaminocyclitol¹⁶ as

Received: March 1, 2018

Published: March 30, 2018

Scheme 1. Synthesis of 1*H*-Imidazoles 6 and 7^a

^aReagents and conditions: (a) RuCl₃·3H₂O (7 mol %), NaIO₄, EtOAc, MeCN, H₂O, 0 °C, 90 min, **11a** 40%, **11b** 32%; (b) MsCl, *N*-methylimidazole, Et₃N, CHCl₃, rt, 16 h, then NaN₃, DMF, 100 °C, 16 h, **12a** 74%, **12b** 58%; (c) PtO₂, H₂, THF, rt, 16 h, **13a** 80%, **13b** 96%; (d) trimethyl orthoformate, HFIP, rt, 16 h, **14a** 76%, **14b** 87%; or trimethyl orthovalerate, HFIP, rt, 16 h, **16a** 74%, **16b** 78%; (e) for **15**: IBX, DMSO, 45 °C, 16 h, 75% from **14a**, 71% from **14b**; for **17**: (COCl)₂, DMSO, DCM, -60 °C, 1 h, 76% from **16a**; 70% from **16b**; (f) Pd(OH)₂/C, H₂, HCl, MeOH, quant. **6**; quant. **7**.

starting material yielded conduritol B-1*H*-imidazoles **8** and **9** (see Supporting Information (SI)).

We determined competitive kinetic constants and IC₅₀ values for 1*H*-imidazoles **6**–**9** as compared with glucoimidazole **5** for inhibition of the retaining glucosidases *Tm*GH1 from *Thermotoga maritima*,²⁰ *Tx*GH116 from *Thermoanaerobacterium xylanolyticum*,²¹ sweet almond β-glucosidase (GH1), human lysosomal acid β-glucosylceramidase (GBA1, GH30), human cytosolic β-glucosylceramidase (GBA2, GH116), murine glucosylceramide synthase (GCS) and human acid α-glucosidase (GAA, GH31). Gluco-1*H*-imidazole **6** displayed micromolar inhibitory activity against most β-glucosidases tested, with *K_i* values ranging from ~3.9 μM against GBA1 to ~69 μM against *Tx*GH116 (Table 1). Remarkably, given their apparent structural similarity, 1*H*-imidazole **6** proved to be

a weaker β-glucosidase inhibitor than glucoimidazole **5**, which inhibited β-glucosidases at nanomolar concentrations. Attachment of a butyl moiety, as in **7**, increased the inhibitory potency of the gluco-1*H*-imidazole scaffold. Though this increase in potency was modest for *Tm*GH1 and *Tx*GH116, **7** inhibited sweet almond β-glucosidase and GBA1 with nanomolar potency. Notably, the biological role of GBA1 is breakdown of amphiphilic glucosylceramide.²² Conduritol-1*H*-imidazole **8** did not effectively inhibit any glucosidases tested except for GBA1, consistent with a loss of interactions at the O6 position, but also with the fact that GBA1 is effectively inhibited by conduritol B epoxide (CBE).²³ As with the gluco-1*H*-imidazoles, addition of a butyl moiety to the conduritol-1*H*-imidazole scaffold increased activity against sweet almond β-glucosidase and GBA1, rendering **9** a nanomolar inhibitor of these enzymes. No compounds displayed any inhibitory activity against GBA2, GCS or α-glucosidase GAA under our assay conditions. Competitive, selective GBA1 inhibitors are considered attractive starting points for the development of pharmacological chaperones: compounds that stabilize the fold of mutant, partially malfunctioning GBA1 in Gaucher patients.^{24,25} Compounds **7** and **9** (as well as known glucoimidazole **5**) are in our opinion attractive starting points for this purpose.

One striking result displayed in Table 1 is that 1*H*-imidazole **6** is a comparatively much weaker retaining β-glucosidase inhibitor than glucoimidazole **5**. Because the structures are closely related, we elected to investigate this result in more depth. Literature studies have shown that the inherent basicity of the azole ring in compounds **2**–**5** correlates to the inhibitory potency.^{26,27} Basicity plays a negligible role here, because the experimental p*K_{AH}* values of **5** and **6** are almost identical (5: p*K_{AH}* 6.2, lit. 6.1;²⁶ **6**: p*K_{AH}* 6.0; Figure S1, S2). We also explored the interaction of gluco-1*H*-imidazoles with *Tm*GH1 and *Tx*GH116 by isothermal titration calorimetry (ITC) at pH 5.8 (activity optimum^{11,21}) and pH 6.8 (where **5** shows strongest inhibition).¹¹ In line with the *K_i* data (Table 1), ITC titrations at both pH values showed nanomolar binding affinities for **5**, and micromolar affinities for **6** and **7** (Table S3). The enthalpic contributions in active site binding for 1*H*-azoles are smaller than those observed for **5**, and only partially compensated for by increased entropic contributions to the binding energy. In line with what has been reported for **5**,¹¹ the presence of a hydrophobic moiety in **7** reduced its enthalpy of binding compared to **6**, which was counterbalanced by an increase in favorable entropic contributions to binding.

Next, the X-ray structure of **6** in complex with *Tm*GH1 was determined to 1.7 Å (PDB: 5OSS), and compared to the structure of the same enzyme complexed with **5** (PDB: 2CES).¹¹ These structures revealed the binding mode of both compounds to be similar. We observed a single molecule of **6** in

Table 1. Inhibition Constants (*K_i*) and IC₅₀ Values in μM for Compounds **5**–**9**

	<i>Tm</i> GH1 ^b	<i>Tx</i> GH116 ^b	sweet almond GH1 ^c	GBA1 ^b	GBA2 ^d	GCS ^d	GAA ^d
6	58 ± 1	69 ± 12	23 ± 1	3.9 ± 2	>100	>50	>100
7	39 ± 14	46 ± 5	0.039 ± 0.006	0.133 ± 0.040	>100	>50	>100
8	>100 ^d	>100 ^d	>100 ^d	13.7 ± 6	>100	>50	>100
9	>100 ^d	>100 ^d	0.221 ± 0.004	0.079 ± 0.001	>100	>50	>100
5	0.026 ± 0.001	0.165 ± 0.006	0.067 ± 0.004 ^e	0.070 ± 0.005	>100	>50	>100

^aValues are mean ± SD from triplicate experiments. ^bAssays measured at pH 6.8 using β-*p*-NPG substrate. ^cpH 5.2 using β-2,4-DNPG substrate. ^dApparent IC₅₀. ^eLit. *K_i* = 0.100 μM.⁶

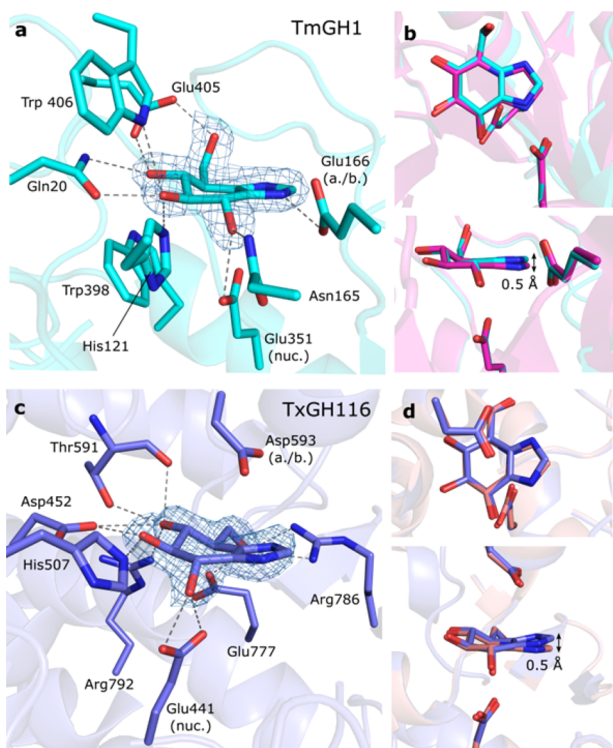


Figure 2. (a) Gluco-1*H*-imidazole **6** in complex with *TmGH1*, with direct H-bonding interactions shown. (b) Overlay of **5** (pink) and **6** (cyan) within the *TmGH1* active site (chain B from each structure). (c) Gluco-1*H*-imidazole **6** in complex with *TxGH116*. (d) Overlay of **5** (salmon) and **6** (blue) within the *TxGH116* active site. Electron densities are REFMAC maximum-likelihood/ σ_A weighted 2Fo–Fc contoured to 0.38 (*TmGH1*) or 0.48 (*TxGH116*) $e^-/\text{\AA}^3$.

the active site after ligand soaking, adopting a 4E conformation, similar to the complex of **5** and *TmGH1* (Figure 2a).¹¹ The H-bonding interactions made by **6** to active site residues were identical to those observed with **5**, albeit with a slight “upward” tilt for **6** compared to **5** (~ 0.4 or 0.5 Å “upward” shifts at the apical imidazole carbon, compared with ligands in chains A or B of 2CES respectively; Figure 2b, Figure S3). Crystal structures in *TxGH116* at 2.1 Å resolution (Figure 2c,d) also revealed similar binding modes²¹ and a ~ 0.5 Å “upward” tilt for **6** compared to **5** (PDB: 5OST and 5BX4, respectively). For both *TmGH1* and *TxGH116* complexes, B-factors in the “imidazole” portion of **6** were markedly higher when compared to the “glucose” portion of the molecule, indicating the imidazole of **6** was more disordered in the crystal structure and may be bound less strongly. No strong B-factor trend was observed for complexes with **5** (Figure S3).

The underlying cause for the reduced potency of gluco-1*H*-imidazole **6** compared to **5** is most likely the combination of a number of factors. We propose that repositioning of the N1 atom (from the bridgehead position in **5** to the position in **6**) brings two major consequences that together reduce the binding affinity of **6** compared to **5**. First, considering the situation where the imidazole is in a neutral state:²⁸ the free lone pair of the N2 atom in **5** can laterally coordinate to the acid/base residue of the bound glucosidase in typical *anti*-protonating glucosidases¹⁴ (although *TxGH116* lacks this interaction due to the unusual placement of its acid/base residue²¹). This lateral positioning of N2 is maintained in **6**, as observed in its complex with *TmGH1* (Figure 2a). However,

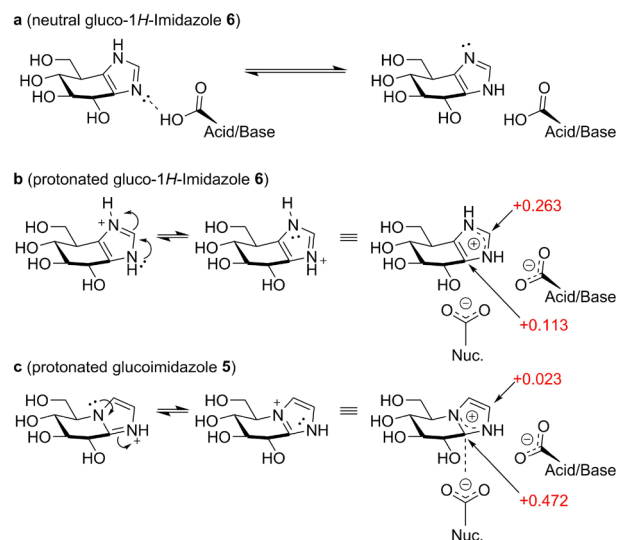


Figure 3. Interactions of gluco-1*H*-imidazole **6** and classical glucoimidazole **5** with the catalytic residues. (a) Prototropic tautomerism of **6**. (b) Positive charge is delocalized onto the “apical” carbon in protonated **6**. (c) In **5**, positive charge is delocalized onto the anomeric equivalent carbon, ideally located for charge–charge interaction with the nucleophile residue. Mulliken charges are annotated in red.

and in contrast to **5**, 1*H*-imidazole **6** may undergo prototropic tautomerism (Figure 3a). Thus, though the overall pK_{AH} values of **5** and **6** are similar, the N2 lone pair of **6** may be less available for interaction with the glucosidase acid/base, reducing the binding affinity of **6** compared to **5**. Protonation of the imidazole in turn (either in solution or by proton abstraction from the acid/base residue)²⁸ results in positive charge delocalization. Resulting charge–charge interactions with enzyme active site carboxylates are thought to contribute substantially to enzyme binding energy of azole-type inhibitors.²⁹ We calculated the Mulliken charge on all atoms for protonated **5** and **6** by DFT. Protonation of theazole ring in **5** produces a $\delta+$ charge on the “anomeric” carbon, which is ideally located for a charge–charge interaction with a retaining glucosidase active site nucleophile. Conversely, protonation of **6** leads to a $\delta+$ charge largely delocalized onto the “apical” carbon atom of the imidazole, with the overall $\delta+$ charge also being less pronounced (Figure 3b). This apical $\delta+$ charge is located distal from the catalytic nucleophile and thus poorly positioned for charge–charge interactions, which may explain the reduced binding enthalpy observed in ITC for gluco-1*H*-imidazoles **6** compared to **5**. The small “upward” shift and increased imidazole B-factors, observed in crystal structure complexes of **6** compared to **5** is also consistent with a weaker charge–charge interaction of the imidazole portion of **6** with the enzyme catalytic nucleophile. Interestingly, in contrast to neutral **6**, glucoimidazole **5** also contains a significant $\delta+$ character (+0.306 Mulliken charge) on the “anomeric” carbon in its neutral state (see SI).

In conclusion, we have described a new class of competitive β -glucosidase inhibitors: the 1*H*-gluco-azoles. The synthetic route is flexible regarding substituents on the imidazole ring, and can likely be transferred to configurational isomers by applying this route to configurational isomers of cyclohexene **10**.³⁰ Our compounds resemble to some extent the 1*H*-imidazoles reported by Li and Byers,³¹ and Field et al.,³² whose

simple, achiral molecules inhibit several glucosidases as well, though likely by a different mode of action. 1*H*-Imidazole **6** appeared a poorer inhibitor than compound **5**, and we hypothesize this is caused by delocalization of the lone pair on the nitrogen atom due to tautomerism and/or impaired δ^+ charge development at the anomeric center. Introduction of an alkyl substituent on the 1*H*-imidazole ring (as in **7**) as well as “deletion” of the methylene carbon (as in **9**) yielded potent competitive inhibitors of the human lysosomal glucosylceramidase GBA1, selective over human cytosolic GBA2 and GCS. These and related compounds we postulate have potential to be developed into pharmacological chaperone candidates for Gaucher disease and perhaps also neuropathological disorders (in particular, Parkinsonism) that are characterized by partial deficiency in GBA.^{33,34}

■ ASSOCIATED CONTENT

📄 Supporting Information

The Supporting Information is available free of charge on the ACS Publications website at DOI: [10.1021/jacs.8b02399](https://doi.org/10.1021/jacs.8b02399).

Experimental data and procedures, enzyme kinetics, DFT calculations, crystallographic data (PDF)

■ AUTHOR INFORMATION

Corresponding Author

*h.s.overkleeft@lic.leidenuniv.nl

ORCID

Marta Artola: [0000-0002-3051-3902](https://orcid.org/0000-0002-3051-3902)

Jeroen D. C. Codée: [0000-0003-3531-2138](https://orcid.org/0000-0003-3531-2138)

Gideon J. Davies: [0000-0002-7343-776X](https://orcid.org/0000-0002-7343-776X)

Herman S. Overkleeft: [0000-0001-6976-7005](https://orcid.org/0000-0001-6976-7005)

Notes

The authors declare no competing financial interest.

■ ACKNOWLEDGMENTS

We thank The Netherlands Organization for Scientific Research (NWO-CW ChemThem grant to J.M.F.G.A. and H.S.O.), the European Research Council (ERC-2011-AdG-290836 “Chembiosphing” to H.S.O., and ERC-2012-AdG-322942 “Glycopoise” to G.J.D.), Sanofi Genzyme (research grant to J.M.F.G.A. and H.S.O. and postdoctoral contract to M.A.) and Diamond Light Source (beamline I03, proposal number mx-13587) for provision of data collection facilities. G.J.D. thanks the Royal Society for the Ken Murray Research Professorship.

■ REFERENCES

- (1) Asano, N. *Glycobiology* **2003**, *13*, 93R.
- (2) Lillelund, V. H.; Jensen, H. H.; Liang, X.; Bols, M. *Chem. Rev.* **2002**, *102*, 515.
- (3) Aoyagi, T.; Suda, H.; Uotani, K.; Kojima, F.; Aoyama, T.; Horiguchi, K.; Hamada, M.; Takeuchi, T. *J. Antibiot.* **1992**, *45*, 1404.
- (4) Tatsuta, K.; Miura, S.; Ohta, S.; Gunji, H. *Tetrahedron Lett.* **1995**, *36*, 1085.
- (5) Ermert, P.; Vasella, A. *Helv. Chim. Acta* **1991**, *74*, 2043.
- (6) Granier, T.; Panday, N.; Vasella, A. *Helv. Chim. Acta* **1997**, *80*, 979.
- (7) Heightman, T. D.; Locatelli, M.; Vasella, A. *Helv. Chim. Acta* **1996**, *79*, 2190.
- (8) Speciale, G.; Thompson, A. J.; Davies, G. J.; Williams, S. J. *Curr. Opin. Struct. Biol.* **2014**, *28*, 1.
- (9) Tankrathok, A.; Iglesias-Fernández, J.; Williams, R. J.; Pengthaisong, S.; Baiya, S.; Hakki, Z.; Robinson, R. C.; Hrmova, M.;

Rovira, C.; Williams, S. J.; Ketudat Cairns, J. R. *ACS Catal.* **2015**, *5*, 6041.

(10) Varrot, A.; Schüle, M.; Pipelier, M.; Vasella, A.; Davies, G. J. *J. Am. Chem. Soc.* **1999**, *121*, 2621.

(11) Gloster, T. M.; Roberts, S.; Perugino, G.; Rossi, M.; Moracci, M.; Panday, N.; Terinek, M.; Vasella, A.; Davies, G. J. *Biochemistry* **2006**, *45*, 11879.

(12) Notenboom, V.; Williams, S. J.; Hoos, R.; Withers, S. G.; Rose, D. R. *Biochemistry* **2000**, *39*, 11553.

(13) Hrmova, M.; Streltsov, V. A.; Smith, B. J.; Vasella, A.; Varghese, J. N.; Fincher, G. B. *Biochemistry* **2005**, *44*, 16529.

(14) Heightman, T. D.; Vasella, A. T. *Angew. Chem., Int. Ed.* **1999**, *38*, 750.

(15) Hansen, F. G.; Bundgaard, E.; Madsen, R. *J. Org. Chem.* **2005**, *70*, 10139.

(16) Trapero, A.; Llebaria, A. *ACS Med. Chem. Lett.* **2011**, *2*, 614.

(17) Artola, M.; Wu, L.; Ferraz, M. J.; Kuo, C. L.; Raich, L.; Breen, I. Z.; Offen, W. A.; Codée, J. D. C.; van der Marel, G. A.; Rovira, C.; Aerts, J. M. F. G.; Davies, G. J.; Overkleeft, H. S. *ACS Cent. Sci.* **2017**, *3*, 784.

(18) Khaksar, S.; Heydari, A.; Tajbakhsh, M.; Vahdat, S. M. *J. Fluorine Chem.* **2010**, *131*, 1377.

(19) Nicolaou, K. C.; Mathison, C. J. N.; Montagnon, T. *J. Am. Chem. Soc.* **2004**, *126*, 5192.

(20) Liu, L.; Zeng, Z.; Chen, M.; Zhang, Y.; Zhang, J.; Fang, X.; Jiang, M.; Lu, L. *Bioorg. Med. Chem. Lett.* **2012**, *22*, 837.

(21) Charoenwattanasatien, R.; Pengthaisong, S.; Breen, I.; Mutoh, R.; Sansanya, S.; Hua, Y.; Tankrathok, A.; Wu, L.; Songsiririthigul, C.; Tanaka, H.; Williams, S. J.; Davies, G. J.; Kurisu, G.; Cairns, J. R. K. *ACS Chem. Biol.* **2016**, *11*, 1891.

(22) Abdul-Hammed, M.; Breiden, B.; Schwarzmann, G.; Sandhoff, K. *J. Lipid Res.* **2017**, *58*, 563.

(23) Grabowski, G. A.; Osiecki-Newman, K.; Dinur, T.; Fabbro, D.; Legler, G.; Gatt, S.; Desnick, R. J. *J. Biol. Chem.* **1986**, *261*, 8263.

(24) Sawkar, A. R.; Cheng, W.-C.; Beutler, E.; Wong, C.-H.; Balch, W. E.; Kelly, J. W. *Proc. Natl. Acad. Sci. U. S. A.* **2002**, *99*, 15428.

(25) Steet, R. A.; Chung, S.; Wustman, B.; Powe, A.; Do, H.; Kornfeld, S. A. *Proc. Natl. Acad. Sci. U. S. A.* **2006**, *103*, 13813.

(26) Panday, N.; Vasella, A. *Synthesis* **1999**, 1999, 1459.

(27) Panday, N.; Canac, Y.; Vasella, A. *Helv. Chim. Acta* **2000**, *83*, 58.

(28) Wang, B.; Olsen, J. I.; Laursen, B. W.; Navarro Poulsen, J. C.; Bols, M. *Chem. Sci.* **2017**, *8*, 7383.

(29) Heightman, T. D.; Vasella, A.; Tsitsanou, K. E.; Zographos, S. E.; Skamnaki, V. T.; Oikonomakos, N. G. *Helv. Chim. Acta* **1998**, *81*, 853.

(30) Harrak, Y.; Barra, C. M.; Delgado, A.; Castaño, A. R.; Llebaria, A. *J. Am. Chem. Soc.* **2011**, *133*, 12079.

(31) Li, Y.-K.; Byers, L. D. *Biochim. Biophys. Acta, Protein Struct. Mol. Enzymol.* **1989**, *999*, 227.

(32) Field, R. A.; Haines, A. H.; Chrystal, E. J. T.; Lusznik, M. C. *Biochem. J.* **1991**, *274*, 885.

(33) Mazzulli, J. R.; Xu, Y. H.; Sun, Y.; Knight, A. L.; McLean, P. J.; Caldwell, G. A.; Sidransky, E.; Grabowski, G. A.; Krainc, D. *Cell* **2011**, *146*, 37.

(34) Gegg, M. E.; Burke, D.; Heales, S. J. R.; Cooper, J. M.; Hardy, J.; Wood, N. W.; Schapira, A. H. V. *Ann. Neurol.* **2012**, *72*, 455.